Available online at www.sciencedirect.com

ScienceDirect

Journal of Taibah University for Science 8 (2014) 385–393

Journal of Taibah University for Science

www.elsevier.com/locate/jtusci

Influence of thermal cycles on thermoelectric uni-leg modules made of $Ca_3Co_4O_9/Ca_{0.95}Sm_{0.05}MnO_3$ oxides

Jérôme Dikwa [a,b,*], Pierre Owono Ateba [b], Simon Quetel-Weben [c], Jean-Marie Bienvenu Ndjaka [b]

[a] *College of Technology, University of Ngaoundere, PO Box 455, Ngaoundere, Cameroon*

[b] *Department of Physics, Faculty of Science, University of Yaounde 1, PO Box 812, Yaounde, Cameroon*

[c] *Laboratoire de Cristallographie et Sciences des Matériaux-Ecole Nationale Supérieure d'Ingénieurs de Caen, Unité mixte de Recherche Centre nationale de Recherche Scientifique 6508, 14050 Caen Cedex, France*

Available online 13 June 2014

Abstract

This paper presents an analysis of the thermoelectric properties of the thermo-elements *p*-$Ca_3Co_4O_9$ and *n*-$Ca_{0.95}Sm_{0.05}MnO_3$ and the diffusion phenomena at the interfaces according to thermal cycle (1, 3 and 7 days at 850 °C). The results show that diffusion at the interfaces is almost nil and is therefore unlikely to be responsible for the poor performance of the modules. The thermoelectric properties of *p*-$Ca_3Co_4O_9$ are strongly degraded with the number of thermal cycles, while those of *n*-$Ca_{0.95}Sm_{0.05}MnO_3$ are not affected.

Keywords: Thermo-element; Oxide; Thermoelectric property; Thermal cycle; Diffusion

1. Introduction

Much research has been conducted on thermoelectricity, or the conversion of heat into electricity (Seebeck effect) and vice versa (Peltier effect), in recent years because of environmental concerns. Thermoelectricity has been reserved for environments that are hostile to humans, and the materials used have had poor performance and operate at low temperatures. In 1911, Altenkirch [1] developed a satisfactory theory of the generation of electricity and refrigeration, in which good thermoelectric materials are those that have a good "figure of merit", *ZT*, a dimensionless coefficient given by: $ZT = (S^2/\rho\lambda)T = PF(1/\lambda)T$, where S is the Seebeck coefficient, λ is the thermal conductivity, ρ is the electrical resistivity, PF is the power factor, and T is the absolute temperature.

Recently, high-temperature applications have been used, and good performance was obtained with new materials based on Te, Sb and Pb [2,3], with *ZT* values close to or greater than unity. Such performance, however, is achieved in a controlled atmosphere, as, in the presence of air, these compounds decompose, mainly by volatilization of some elements. In this context, oxides, which may have good performance, are chemically and physically stable at high temperatures as well as in air and may be interesting candidates. Use of oxides as constituents of thermoelectric conversion devices has been

* Corresponding author at: College of Technology, University of Ngaoundere, PO Box 455, Ngaoundere, Cameroon.
Tel.: +237 77 95 78 43/94 75 93 35.
E-mail addresses: jeromedikwa@gmail.com, jerome.dikwa@univ-ndere.cm (J. Dikwa).

Peer review under responsibility of Taibah University

Production and hosting by Elsevier

1658-3655
http://dx.doi.org/10.1016/j.jtusci.2014.05.003

considered only recently, as their narrow conduction bandwidth due to the ionic character of the bonds and pronounced localization of conduction electrons resulting from the strong polarization of the bonds, leading to low carrier mobility, are in complete contradiction to the criteria used to date for choosing thermoelectric materials.

Ohtaki [4] reported *ZT* values of some oxides that indicate the usefulness of the thermoelectric properties of this family of materials. Values close to 1 have been obtained for single crystals. The characteristics of these materials are often limited by their low electrical conductivity, resulting from the low mobility. Studies have been performed on p-type cobalt oxides with a lamellar structure, namely $Ca_3Co_4O_9$, $NaxCoO_2$ and related compounds. These appear to be the best p-type oxide materials, with *ZT* values close to or greater than 1 (for monocrystals) [5–7]. $Ca_3Co_4O_9$ was studied by Prevel et al. [8], and use of these elements in some modules was reported by Urata et al. [9] and Choi et al. [10].

Another family of materials, manganites, has been studied for thermoelectric properties. Although the *ZT* values obtained are lower, some compounds, such as $Ca_{1-x}Bi_xMnO_3$ and $Ca_{1-x}Sm_xMnO_3$, have been integrated into such devices [11–13]. In these materials, electrical conductivity and the Seebeck coefficient vary like those of metals. With the compound $Ca_{0.9}Yb_{0.1}MnO_3$, Flahaut obtained $ZT = 0.16$ at 1000 K [14], making manganite $Ca_{1-x}TR_xMnO_3$ the highest performing *n*-type oxide.

Although the *ZT* of materials has improved, increasing the performance of thermoelectric generators, the performance often decreases with the number of operating cycles [9,15]. To investigate this phenomenon, we synthesized $Ca_3Co_4O_9$ and $Ca_{0.95}Sm_{0.05}MnO_3$ and subjected them to a conventional sintering process. We then developed one-leg modules that undergo cycles of 1 day, 3 days and 7 days at 850 °C and compared the thermoelectric properties as a function of annealing cycles. We also studied the diffusion phenomena at the interface by scanning electron microscopy coupled with energy dispersive X-ray spectrometry.

2. Experimental

2.1. Synthesis

Aliquots of 20 g of $Ca_3Co_4O_9$ powder were synthesized by conventional solid-state synthesis from a mixture prepared in stoichiometric proportions [8] of 12.8435 g Co_3O_4 (Analor Normapur-Prolabo) and 12.0114 g $CaCO_3$ (Cerac, 99.95%). The elements were mixed under dry conditions in a spray set to 400 rpm for 30 min; then, the mixture was finely crushed in a mortar and calcined at 900 °C for 24 h to promote decomposition of the carbonates and to obtain the $Ca_3Co_4O_9$ phase according to the following equation:

$$\tfrac{4}{3}Co_3O_4 + 3CaCO_3 + \tfrac{1}{3}O_2 \rightarrow Ca_3Co_4O_9 + 3CO_2 \quad (1)$$

To synthesize manganite $Ca_{0.95}Sm_{0.05}MnO_3$, we used the co-precipitation synthesis method, which, according to Lemmonier et al. [11], provides the best thermoelectric properties. The solution of calcium, manganese and samarium (prepared by reductive acid attack of calcium and manganese carbonates) was poured into a solution of ammonium carbonate, and the resulting precipitate was filtered, dried and calcined.

For synthesis of 10 g of $Ca_{0.95}Sm_{0.05}MnO_3$ powder, we used 6.45 g $CaCO_3$ (Diopma, 99.99%), 7.74 g $MnCO_3$ (Cerac, 99.95%), 1.5 g ($Sm(NO_3)_3$, $6H_2O$) (Alfa Aesar, 99.9%), approximately 30 ml HNO_3 65% (VWR), approximately 1.5 ml H_2O_2 110 vol (Acros, 35%) and 78 g NH_4HCO_3 (VWR).

The precursor salts $CaCO_3$, $MnCO_3$ and ($Sm(NO_3)_3$, $6H_2O$) were mixed in an aqueous solution in stoichiometric proportions. To accelerate dissolution of the compounds, the solution was heated to 70 °C, and a solution of nitric acid at 65% was added. To avoid precipitation of manganese in MnO_2, a few drops of H_2O_2 were added to reduce Mn^{4+} to Mn^{2+} according to the equation:

$$H_2O_2 + MnO_2 \rightarrow Mn^{2+} + 2H^+ \quad (2)$$

After the last addition, all components were in aqueous form and it was possible under some conditions to precipitate $Ca_{0.95}Sm_{0.05}Mn(CO_3)_2$. The precipitating solution consisted of an aqueous solution of $NH_4)_2CO_3$ at 0.4 mol/L. Endothermic dissolution of the salts reduced the temperature of the solution, and the solution containing the precursor was then slowly poured into the precipitating solution. Crystallization was rapid, with ripening of the solution for about 2 h under mechanical and ultrasonic agitation, then vacuum filtering through a Buchner funnel. The material was dried at 100 °C in an oven for about 6 h, and the precipitate was calcined in a porcelain crucible at 850 °C for 6 h under air, the porcelain crucible being introduced into a furnace in which the speed of change of temperature was set to 150 °C/h. To determine the ideal temperature of calcination, X-ray diffraction was conducted at various temperatures.

2.2. Shaping and sintering

Before sintering, the crucial step is shaping, which allows good cohesion of grains and better distribution of the material to eliminate intergranular porosity. We used the uniaxial pressing method for shaping bars. The powder was inserted into a cylindrical or parallelepiped mould between two piston pellets, and the powder was compacted vertically by the upper piston. For preparation of $Ca_3Co_4O_9$ bars, a few drops of binder (polyvinyl alcohol polymer, Rhodoviol 5%) were added to 1.2 g of powder; the whole sample was ground in a mortar, then dried and reground. The resulting powder was divided into four portions of 0.3 g, which were introduced into the four compartments of a uniaxial press mould with the press set to 110 mV and 44.3 kN. The bars were recovered and sintered in a furnace at 920 °C for 24 h in air. $Ca_{0.95}Sm_{0.05}MnO_3$ bars were prepared in the same manner, except that sintering was done at 1200 °C for 6 h.

2.3. Chemical and structural characterization

Phase identification was conducted by X-ray diffraction in Xpert Pro MPD PANalytical (bla) and D8 Advance Vario 1 Bruker diffractometers. The latter can be used at high temperature and is based on a Bragg–Brentano protocol θ–2θ, the main characteristic being the constant distance between the sample and the detector regardless of the θ angle. The different crystalline phases present in samples were determined precisely by comparing the X-ray diffraction patterns to referenced phases of the Xpert Highscore software. Lattice parameters were determined accurately with Jana 2006 software [16], which is based on the Rietveld method [17] for accurate determination of the lattice parameters of the crystal structure.

Microstructural studies were performed under a Carl Zeiss scanning electron microscope (Supra 55, Oberkochen, Germany) after polishing stages with abrasive discs. Diffusion at metal–oxide interfaces was investigated by scanning electron microscopy coupled with energy dispersive X-ray spectrometry.

2.4. Thermoelectrical characterization at high temperature

The temperature dependence of electrical resistivity (ρ) and the Seebeck coefficient (S) was measured simultaneously in a direction perpendicular to the pressure axis, in a ZEM-3 apparatus (ULVACRIKO Inc., Japan) in the temperature range 100–600 °C. Measurements were performed on ~2.5 mm × 2.5 mm × 10 mm bar-shaped samples at low-pressure helium. Both ends of the bar were polished so that they were parallel, in order to ensure good contact with the nickel electrodes of the device. The temperature of the measuring chamber was increased from room temperature to 600 °C in a halogen oven controlled by temperature probes (Yamatake, model SDC30), which also measure the sample temperature.

2.5. Uni-leg modules

We developed uni-leg modules to study diffusion at the interfaces. The interconnected metal was the silver blade, and contact between the silver blade and the thermoelement was ensured by silver lacquer. A silver blade was chosen as the interconnected metal because silver is a good conductor and has a higher melting-point than platinum, which is very expensive and rare.

The completed modules were annealed in air in a furnace at 900 °C for 12 h to solidify the contacts. Before the annealing phase, modules were preheated to 100 °C for 6 h in an oven under load, to permit vaporization of the solvent in the lacquer in order to ensure good adhesion at the interface.

3. Results and discussion

Fig. 1 shows the X-ray diffraction patterns of a $Ca_3Co_4O_9$ bar sample prepared by conventional sintering. The calcination performed at 900 °C during 24 h is essentially a decarbonation step; it does not allow complete formation of the $Ca_3Co_4O_9$ phase, which requires the sintering step to obtain pure ceramic compound.

X-ray diffraction results in comparison with the $Ca_3Co_4O_9$ reference compound did not reveal the presence of secondary phases. After Rietveld refinement, however, the lattice parameters $a = 4.8912(4)$ Å, $b = 36.336(4)$ Å, $c = 10.8226(3)$ Å, $\alpha = 90°$, $\gamma = 90°$ and $\beta = 98.809(3)°$ were consistent with the values commonly reported for polycrystalline $Ca_3Co_4O_9$ [8] (Fig. 1).

In order to determine the ideal temperature for calcination of precursors synthesized by co-precipitation to obtain pure $Ca_{0.95}Sm_{0.05}MnO_3$, X-ray diffraction patterns were obtained at various temperatures (Fig. 2) with the D8 diffractometer. X-ray diffraction after drying revealed a single phase of $Ca_{0.95}Sm_{0.05}Mn(CO_3)_2$ carbonate. In that form, the manganese atom has only one degree of oxidation, which we found to be 2. Pure phase $Ca_{0.95}Sm_{0.05}MnO_3$ was obtained only at a temperature of 850 °C or above.

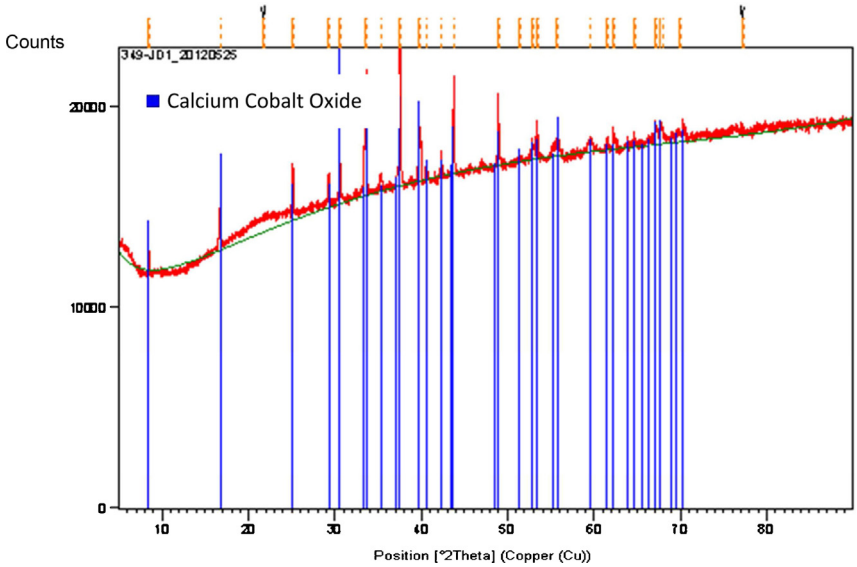

Fig. 1. X-ray diffraction patterns of $Ca_3Co_4O_9$ prepared by conventional sintering.

Fig. 3 shows an X-ray diffractogram of the $Ca_{0.95}Sm_{0.05}MnO_3$ powder obtained after calcination at 850 °C. The image does not reveal the presence of secondary phases; however, after Rietveld refinement, the resulting lattice parameters $a = 5.27253(4)$ Å, $b = 7.44412(3)$ Å and $c = 5.26871(2)$ Å are consistent with the values referenced in the software and those reported by Lemmonier et al. [11] for the polycrystalline compound $Ca_{0.95}Sm_{0.05}MnO_3$. Synthesis by co-precipitation is thus suitable for obtaining pure phase $Ca_{0.95}Sm_{0.05}MnO_3$.

Fig. 4 shows the resistivity of various samples of *p*-$Ca_3Co_4O_9$ and *n*-$Ca_{0.95}Sm_{0.05}MnO_3$ annealed at 850 °C for 1, 2 or 3 days. The resistivity of $Ca_3Co_4O_9$ annealed for 1 day decreased with temperature, suggesting that it has semiconductor behaviour. The resistivity increased with thermal cycles of annealing, the increase being more pronounced at low temperatures, while the resistivity

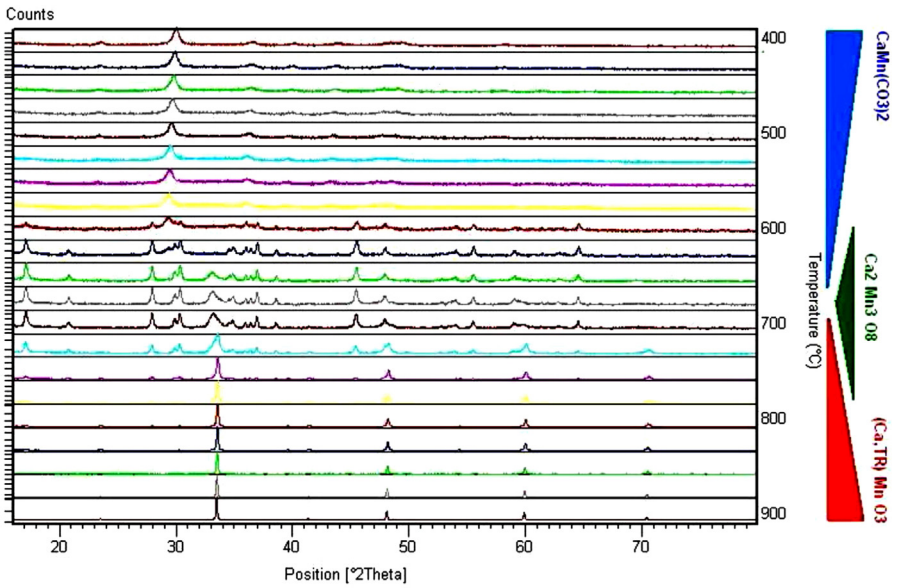

Fig. 2. X-ray diffractograms showing calcination temperature of precursors synthesized by co-precipitation.

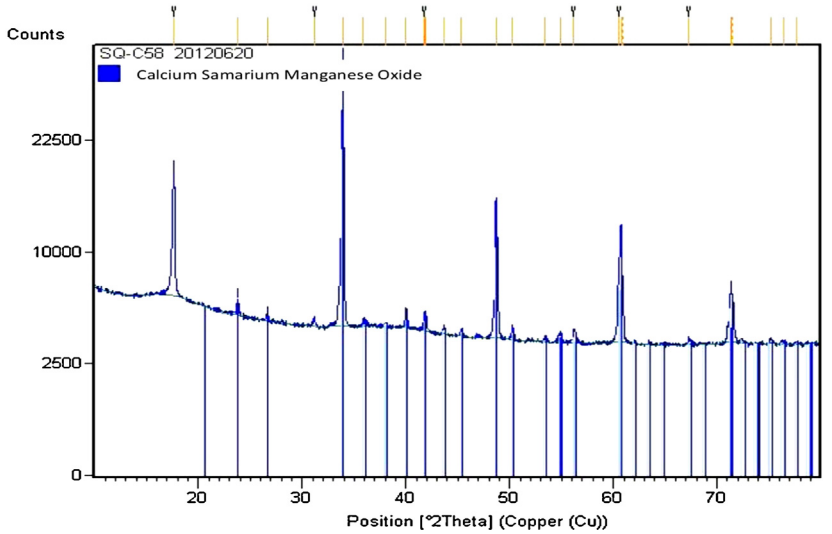

Fig. 3. X-ray diffractogram of $Ca_{0.95}Sm_{0.05}MnO_3$ powder after calcination at 850 °C.

curves converged at high temperatures. The number of thermal cycles had a detrimental effect on the electrical conductivity ($\sigma = 1/\rho$) of $Ca_3Co_4O_9$ compounds, as seen by the appearance of micro-cracks, which would create barriers to charge carriers (holes e^+) and have less effect at high temperatures. This assumption was confirmed later by X-ray analysis of $Ca_3Co_4O_9$ annealed for 7 days. The increase in electrical resistivity cannot be attributed to decomposition of the $Ca_3Co_4O_9$ phase, because the annealing temperature of 850 °C is much lower than the decomposition temperature of the $Ca_3Co_4O_9$ phase, which is 926 °C.

For the $Ca_{0.95}Sm_{0.05}MnO_3$ compound, we observed no variance in resistivity with the number of thermal cycles or with temperature, indicating that $Ca_{0.95}Sm_{0.05}MnO_3$ has a metallic type behaviour.

Fig. 5 shows the temperature dependence of the Seebeck coefficient (thermopower) of annealed samples of p-$Ca_3Co_4O_9$ and n-$Ca_{0.95}Sm_{0.05}MnO_3$. For $Ca_{0.95}Sm_{0.05}MnO_3$, the Seebeck coefficient did not vary with the number of thermal cycles. The decrease with temperature confirms that this compound has a metallic type behaviour. Negative values of the Seebeck coefficient show that the charge carriers are electrons (e^-) and that this compound is n-type. For $Ca_3Co_4O_9$, the curves show that the Seebeck coefficient was not very sensitive to the number of thermal cycles and that it increased with temperature. Unlike those for the $Ca_{0.95}Sm_{0.05}MnO_3$

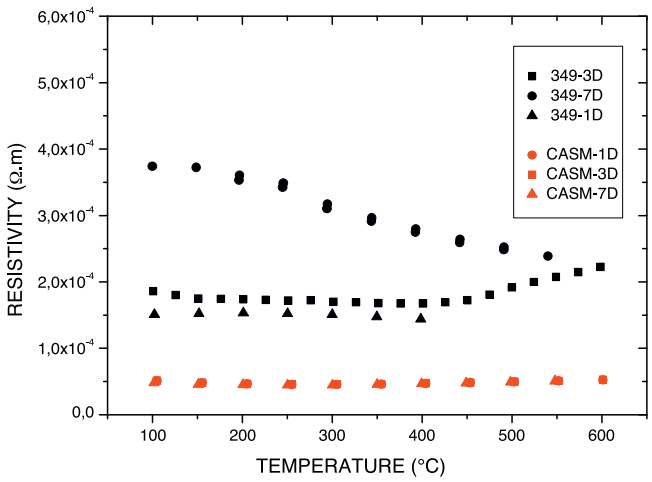

Fig. 4. Curves of resistivity after annealing at 850 °C for 1, 3 or 7 days.

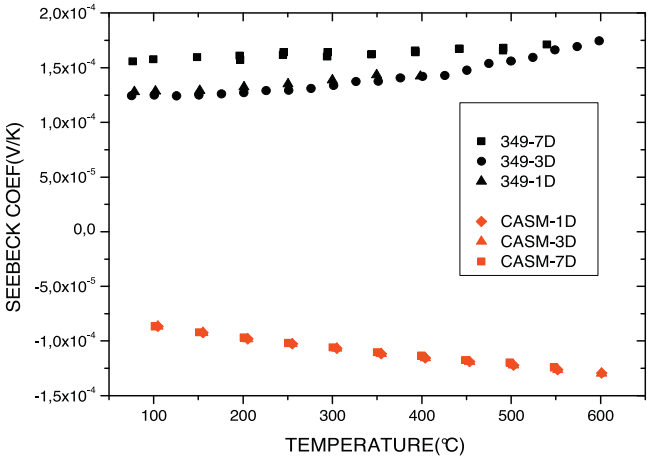

Fig. 5. Seebeck coefficient curves after annealing at 850 °C for 1, 3 or 7 days.

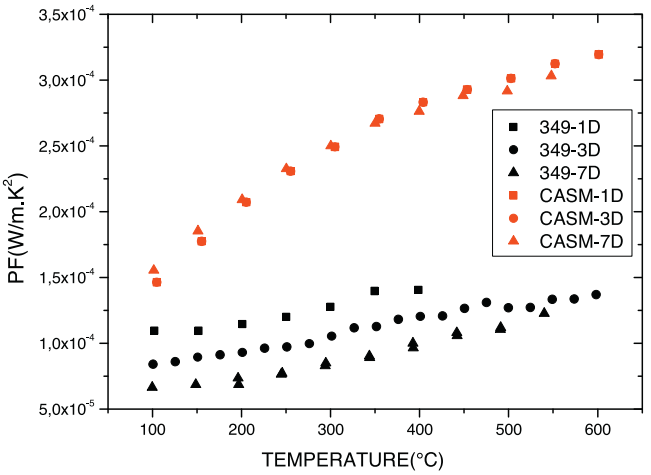

Fig. 6. Power factor curves after annealing at 850 °C for 1, 3 or 7 days.

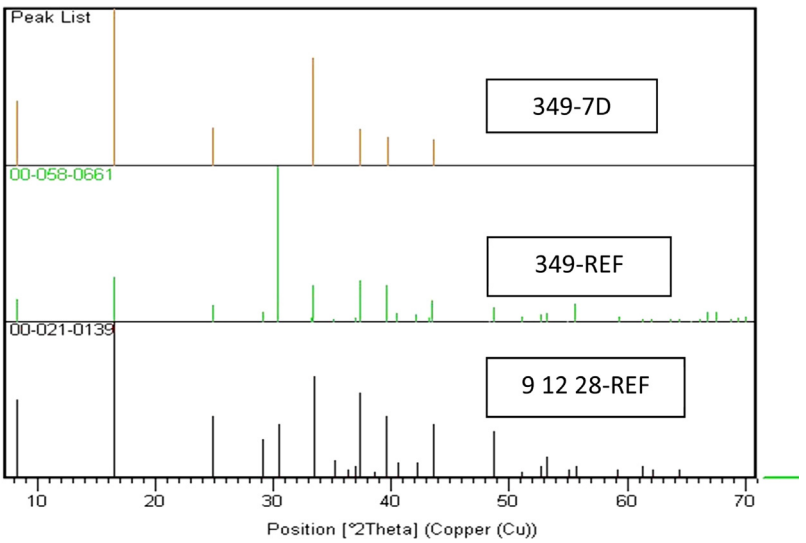

Fig. 7. X-ray diffraction patterns of $Ca_3Co_4O_9$ annealed at 850 °C for 7 days and of $Ca_3Co_4O_9$ and $Ca_9Co_{12}O_{28}$ reference phases.

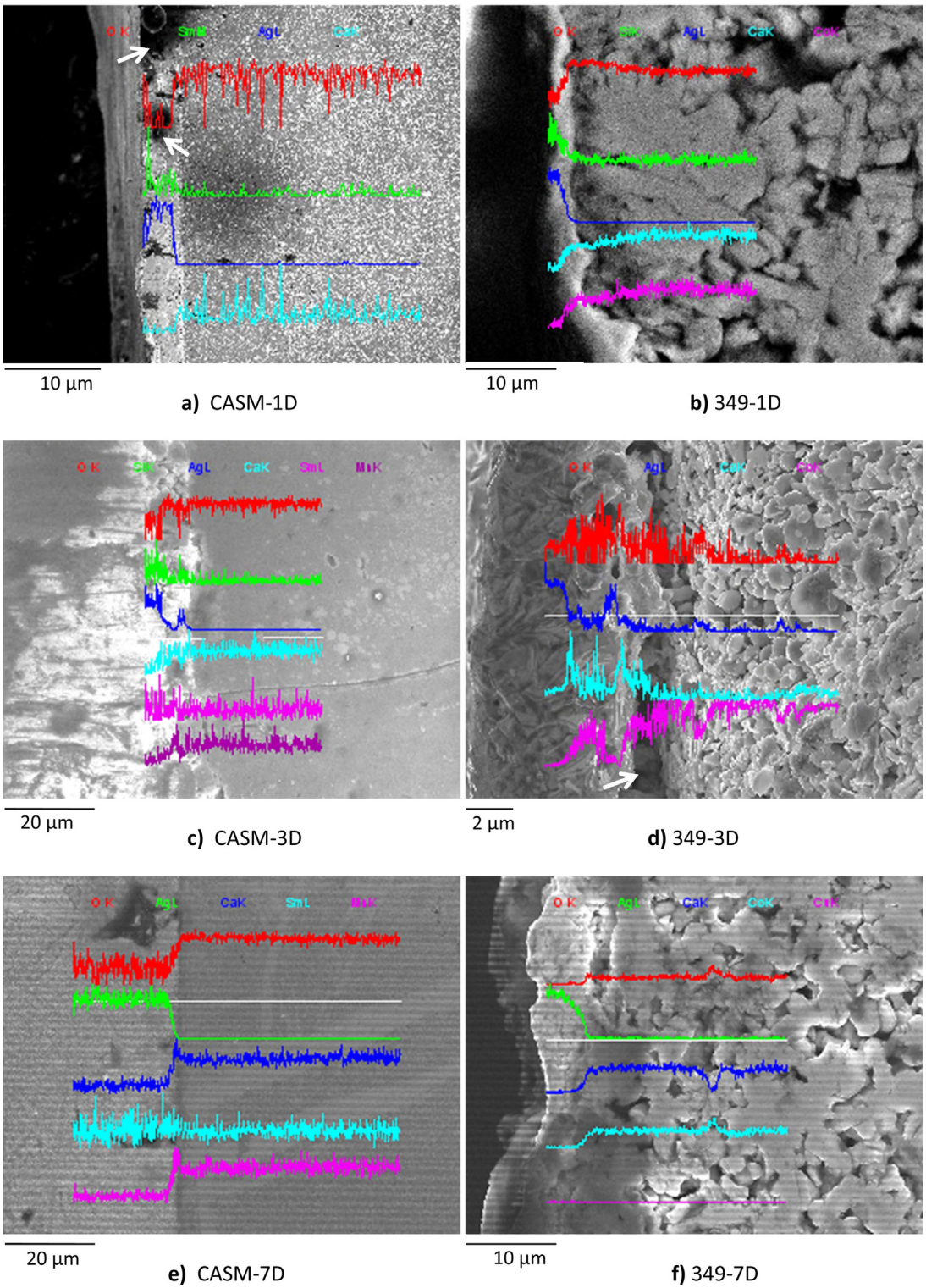

Fig. 8. Scanning electron microscopy coupled with energy dispersive X-ray spectrometry of diffusion at interfaces. (a) *n*-$Ca_{0.95}Sm_{0.05}MnO_3$-1D; (b) $Ca_3Co_4O_9$ annealed for 1 day; (c) *n*-$Ca_{0.95}Sm_{0.05}MnO_3$ annealed for 3 days; (d) $Ca_3Co_4O_9$ annealed for 3 days; (e) *n*-$Ca_{0.95}Sm_{0.05}MnO_3$ annealed for 7 days; and (f) $Ca_3Co_4O_9$ annealed for 7 days.

compound, the coefficients for $Ca_3Co_4O_9$ were positive, confirming that the charge carriers in this material are holes (e^+) and that this compound is *p*-type.

Fig. 6 shows the temperature dependence of the power factor (*PF*) for the annealed samples. As the electrical resistivity (ρ) and the Seebeck coefficient (*S*) of the *n*-type thermo-elements $Ca_{0.95}Sm_{0.05}MnO_3$ are insensitive to the number of thermal cycles, the power factor ($PF = \sigma^2/\rho$) is also invariant. The *n*-type oxide $Ca_{0.95}Sm_{0.05}MnO_3$ is therefore stable during cycles of use, and the increase in the power factor with temperature indicates its possible performance.

Furthermore, the resistivity (ρ) of $Ca_3Co_4O_9$ increased with no substantial increase in the Seebeck coefficient; therefore, its power factor is considerably degraded with increasing numbers of thermal cycles. As the figure of merit $ZT = PF \cdot 1/\lambda T$ is proportional to the power factor, the decrease in *PF* results in a decrease in *ZT*, i.e. a decrease in the performance of $Ca_3Co_4O_9$ and of thermoelectric generators made up of the pair *p*-$Ca_{2.7}Bi_{0.3}Co_4O_9$/*n*-$CaMn_{0.98}Mo_{0.02}O_3$ according to the number of cycles of use. These results are contrary to those of Urata et al. [9], who reported a deterioration of the *p*-type leg on thermoelectric generators made up of this pair. They attributed the decrease in performance to a difference in expansion of the *p*- and *n*-type thermo-elements and to a significant increase in contact resistance, as suggested in 1998 by Rowe and Min [15]. To overcome the difference in thermal expansion, we studied two separate thermo-elements.

The degradation of the thermoelectric properties of $Ca_3Co_4O_9$ samples prompted us to study the sample annealed for 7 days, whose properties were the most degraded. The diffraction patterns obtained are represented in Fig. 7 in comparison with the reference phases of $Ca_9Co_{12}O_{28}$ and $Ca_3Co_4O_9$, because Li et al. [18] showed that the phases of these two compounds are isostructural. The diffraction patterns of $Ca_3Co_4O_9$ annealed for 7 days matched those of $Ca_3Co_4O_9$ phase, indicating that the phase annealed for 7 days was not degraded. Therefore, degradation of the thermoelectric properties of $Ca_3Co_4O_9$ is due to cracking induced by mechanical stress caused by the annealing thermal cycles.

We also performed scanning electron microscopy coupled with energy dispersive X-ray spectrometry of the diffusion at metal–oxide interfaces of the modules after the annealing cycles (Fig. 8) because these materials are intended for use at high temperatures. The analysis showed no trace of diffusion, but rather the presence of porosity, as shown by the arrows in Fig. 8. Therefore, diffusion at interfaces cannot be responsible for the decrease in performance of thermo-generators with increasing cycles of use. The presence of porosity shows that the metal–oxide interface is a sensitive, critical step for the performance of the entire conversion device. Improvement of the contact requires study and optimization of the material used. Thermo-generators with intimate physical contact and good reproducibility of contacts must be developed.

Fig. 8d shows an image obtained by scanning electron microscopy at high magnification on a surface covering both sides of the interface between the interconnecting metal and the thermo-element $Ca_3Co_4O_9$ sintered conventionally. The right side of the interface shows small grains in the form of platelets, which appear to be weakly assembled and oriented randomly. We also saw the presence of a large number of pores, which significantly reduces the density of the material and therefore affects the properties of these ceramics.

4. Conclusion

We synthesized the thermoelectric compounds *p*-$Ca_3Co_4O_9$ and *n*-$Ca_{0.95}Sm_{0.05}MnO_3$ and formed bars of these compounds in the form of thermo-elements by uniaxial pressing and conventional sintering in a furnace. Synthesis by the solid route was effective for obtaining the pure $Ca_3Co_4O_9$ phase, while the pure $Ca_{0.95}Sm_{0.05}MnO_3$ compound was obtained by co-precipitation. Uni-leg modules were developed, and their thermoelectric properties as a function of the number of thermal cycles of annealing at 850 °C were studied for 1, 3 and 7 days. Diffusion at metal–oxide interfaces was studied by scanning electron microscopy coupled with energy dispersive X-ray spectrometry.

We can conclude that the decrease in performance of the thermoelectric generators from *p*-$Ca_3Co_4O_9$/*n*-$Ca_{0.95}Sm_{0.05}MnO_3$ is due to degradation of the thermoelectric properties of $Ca_3Co_4O_9$ during thermal cycling. Other additives must therefore be incorporated into $Ca_3Co_4O_9$, not only to increase the figure of merit but also to ensure thermo-mechanical stability through thermal cycles.

Acknowledgements

The authors thank all the staff of the Laboratoire de Cristallographie et Sciences des Matériaux-Ecole Nationale Supérieure d'Ingénieurs de Caen for allowing completion of the experiment. They especially thank the Functional Materials and Structure group and particularly Jerome Lecourt, technician in the Laboratoire

de Cristallographie et Sciences des Matériaux for his availability and dedication.

References

[1] E. Altenkirch, Physik Z 12 (1911) 920.
[2] K.F. Hsu, S. Loo, F. Guo, W. Chen, J.S. Dyck, C. Uher, T. Hogan, E.K. Polychroniadis, M.G. Kanatzidis, Science 303 (2004) 818.
[3] P.F.P. Poudeu, J. D'Angelo, A.D. Downey, J.L. Short, T.P. Hogan, M.G. Kanatzidis, Angew. Chem. Int. 45 (2006) 3835.
[4] M. Ohtaki, Oral presentation, in: 2nd Workshop on Anisotropic Materials, Gebze (Turkey), 2008.
[5] R. Funahashi, I. Matsubara, H. Ikuta, T. Takeuchi, U. Mizutani, S. Sodeoka, Jpn. J. Appl. Phys. 39 (2000) 1127.
[6] M. Shikano, R. Funahashi, Appl. Phys. Lett. 82 (2003) 1851.
[7] T. Okuda, K. Nakanishi, S. Miyasaka, Y. Tokura, Phys. Rev. B 63 (2001) 113104.
[8] M. Prevel, B. Ouladdiaf, J.G. Noudem, S. Lemonnier, Y. Klein, S. Hébert, D. Chateigner, J. Appl. Phys. 98 (2005) 093706.
[9] S. Urata, R. Funahashi, T. Mihara, A. Kosuga, S. Sodeoka, T. Tanaka, Int. J. Appl. Ceram. Technol. 4 (2007) 535.
[10] S.-M. Choi, K.-H. Lee, C.-H. Lim, W.-S. Seo, Energy Convers. Manage. 52 (2011) 335.
[11] S. Lemmonier, C. Goupil, J.G. Noudem, E. Guilmeau, J. Appl. Phys. 104 (2008) 014505.
[12] I. Matsubara, R. Funahashi, T. Takeuchi, S. Li, K. Ueno, S. Sodeoka, ICT 2000 Proceedings, 2000.
[13] E. Sudhakar Reddy, J.G. Noudem, S. Hebert, C. Goupil, J. Phys. D: Appl. Phys. 38 (2005) 3751.
[14] D. Flahaut, T. Mihara, R. Funahashi, N. Nabeshima, K. Lee, H. Ohta, K. Koumoto, J. Appl. Phys. 100 (2006) 084911.
[15] D.M. Rowe, G. Min, J. Power Source 73 (1998) 193.
[16] V. Petriek, M. Dusek, L. Palatinus, The Crystallographic Computing System, Institute of Physics, Prague, 2006.
[17] H.M. Rietveld, Acta Crystallogr. 22 (1967) 151.
[18] S. Li, R. Funahashi, I. Matsubara, K. Ueno, H. Yamada, J. Mater. Chem. 9 (1999) 1659.